Direct and indirect methods for determination of mode I fracture toughness using PFC^{2D}

Vahab Sarfarazi[*1], Hadi Haeri[**2] and Alireza Bagher Shemirani[3,4]

[1]*Department of Mining Engineering, Hamedan University of Technology, Hamedan, Iran*
[2]*Department of Civil Engineering, Aria University of Sciences and Sustainability, Tehran, Iran*
[3]*Department of Civil Engineering, SADRA Institute of Higher Education, Tehran, Iran*
[4]*Department of Civil Engineering, Sharif University of Technology, Tehran, Iran*

Abstract. In this paper, mode I fracture toughness of rock was determined by direct and indirect methods using Particle Flow Code simulation. Direct methods are compaction tension (CT) test and hollow centre cracked quadratic sample (HCCQS). Indirect methods are notched Brazilian disk (NBD) specimen, the semi-circular bend (SCB) specimen, hollow centre cracked disc (HCCD), the single edge-notched round bar in bending (SENRBB) specimen and edge notched disk (END). It was determined that which one of indirect fracture toughness values is close to direct one. For this purpose, initially calibration of PFC was undertaken with respect to data obtained from Brazilian laboratory tests to ensure the conformity of the simulated numerical models response. Furthermore, the simulated models in five introduced indirect tests were cross checked with the results from direct tests. By using numerical testing, the failure process was visually observed. Discrete element simulations demonstrated that the macro fractures in models are caused by microscopic tensile breakages on large numbers of bonded discs. Mode I fracture toughness of rock in direct test was less than other tests results. Fracture toughness resulted from semi-circular bend specimen test was close to direct test results. Therefore semi-circular bend specimen can be a proper test for determination of Mode I fracture toughness of rock in absence of direct test.

Keywords: tensile strength; direct test; flexural test; double punch tensile test and ring test

1. Introduction

Fracture mechanics is an important parameter in problems relating to rock strength in rock engineering. A fundamental feature of rock fracture mechanics lies in its ability to establish the relationship between rock fracture strength to the geometry of a crack or cracks and the fracture toughness, the most fundamental parameter in fracture mechanics describing resistance of a material to crack propagation. It follows that for quasi-brittle geological materials, crack propagation is the major cause of material failure in many cases. Thus, assessment of fracture toughness is important to the understanding of behaviour of structures involving geological materials. In addition, rock fracture toughness has been applied as a parameter for classification of rock materials, an index for rock fragmentation process and a material property in the interpretation of geological features and in stability analysis of rock structures, as well as in modelling of fracturing in rock. A number of standard methods have been proposed to determine the mode I fracture toughness of rock. They include those based on chevron bend (CB) specimen and

notched Brazilian disk (NBD) specimen, the semicircular bend (SCB) specimen, short rod (SR) specimen, hollow centre cracked disc (HCCD), the single edge-notched round bar in bending (SENRBB) specimen, edge notched disk (END), hollow centre cracked quadratic sample (HCCQS) and Compact tension (CT) test (Barker 1977, Ouchterlony 1980, Atkinson 1982, Shiryaev and Kotkis 1982, Chong and Kuruppu 1984, Huang 1985, Ouchterlony 1986, Banks-Sills 1986, Buchholz 1987, Chong 1987, Ouchterlony 1988, Mahajan 1989, Maccagno 1989, He 1990, Suresh 1990, Singh 1990, Karfakis and Akram 1993, Lim *et al.* 1993, 1994, Khan 2000, Molenar *et al.* 2002, Chang 2002, Sato 2006, Obara *et al.* 2007, 2009, 2010, ISRM 2007, Ayatollahi and Aliha 2007, Dai *et al.* 2010, Kataoka 2011, Tutluoglu 2011, Amrollahi *et al.* 2011, Aliha *et al.* 2008, 2012a, 2012b, 2013, 2014a, 2014b, 2015a, 2015b, Zhou *et al.* 2012, Kataoka 2012, 2013, Ramadoss 2013, Ayatollahi and Alborzi 2013, Kuruppu *et al.* 2014, Pan 2014, Kequan 2015, Lee 2015, Akbas 2016, Rajabi 2016, Haeri *et al.* 2014, Haeri *et al.* 2015a, 2015b, 2015c, Haeri 2015d, 2015e, 2015f, Haeri and Sarfarazi 2016a, Haeri *et al.* 2016b, Mohammad 2016, Fayed 2017). The NBD, SBC, HCCD and CT ISRM-suggested method for mode I fracture toughness determination of rock is herein presented. The CT, HCCQS, SENRBB, SBC, NBD, SENRBB, HCCD and END ISRM-suggested method for mode I fracture toughness determination of rock is herein presented.

CT test

∗Corresponding author, Assistant Professor
E-mail: vahab.sarfarazi@gmail.com or Sarfarazi@hut.ac.ir
∗∗Corresponding author, Assistant Professor
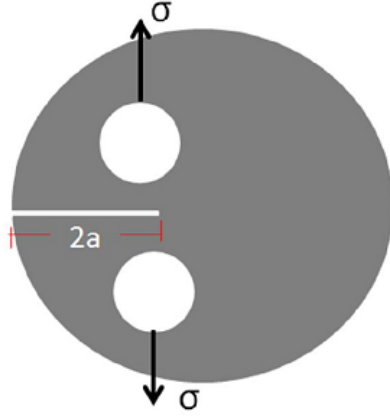E-mail: haerihadi@gmail.com or hadihaeri@otaria.ac.ir
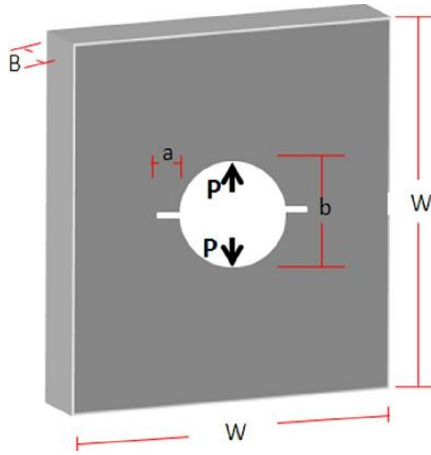
Fig. 1 Compact tension test

Fig. 2 Proposed specimen geometry and test set up loading configuration

Fig. 3 Schematic diagrams of SENRBB specimen

Table 1 Values of $a=D$ and corresponding value of YI from Isida *et al.* (1979)

a/D	0.1	0.2	0.3	0.4	0.5	0.6
F	11.48	7.72	7.05	7.45	8.63	10.99

Fig. 4 Edge notched disk specimen and loading geometry

Compact tension (Sato 2006) test is other method for determination of fracture toughness of material. The fracture toughness of material is determined by applying the tensile load on the crack surface (Fig. 1). The fracture toughness was determined by follow equation

$$K_I = 1.12\, \sigma \sqrt{\pi a} \qquad (1)$$

Where K_I is the mode-I stress intensity factor, σ is the far field stress at failure, a is the half-crack

HCCQS test

Schematic view and geometrical dimension of HCCQS was presented in Fig. 2 (Hadei 2016). As can be seen in Fig. 1(c), HCCD is a quadrangular sample with length (W) of 13 cm and thickness (B) of 2.75 cm. a hole with radius of $b=6$ cm is drilled in the centre of the sample. Two straight central cracks with length of $a=6$ mm are created from the surface of the hole. These cracks are perpendicular with loading axis (P). The stress intensity factors (KI) mode I for the HCCQS specimen is often written as

$$K_I = YI \frac{P}{2bB} \sqrt{\pi a} \qquad (2)$$

Where P is applied tensile load and YI is non-dimensional stress intensity factor.
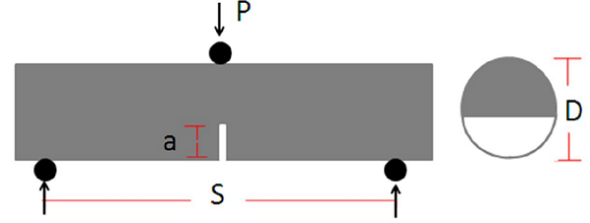
$$YI = 596.1(a/b)^4 - 785.9(a/b)^3 + 372.3(a/b)^2 - 68.3\left(\frac{a}{b}\right) + 8.271 \qquad (3)$$

SENRBB test

For the SENRBB specimen (Fig. 3), the fracture toughness, *KIC*; is determined using the peak load (P), the non-dimensional stress intensity factor, and the specimen dimensions (Ouchterlony 1981). *KIC* may be given as

$$KIC = 0.25\left(\frac{S}{D}\right) YI \frac{F_{max}}{D^{1.5}} \qquad (4)$$

Where YI is the non-dimensional stress intensity factor, F max is the maximum load, S is the span length between the two support rollers, and D is the specimen diameter. The non-dimensional stress intensity factor YI is given by

$$YI = 2\left(\frac{D}{s}\right)\left[450.8531P^2\left(\frac{a}{D}\right)^{1.5}\right] / [(a/D) - (a/D)^2]^{0.25} \qquad (5)$$

END test

Schematic view and geometrical dimension of END is presented in Fig. 4 (Isida 1979). As can be seen in Fig. 1(c), END is a disc with diameter of D and thickness (B) of 2.75
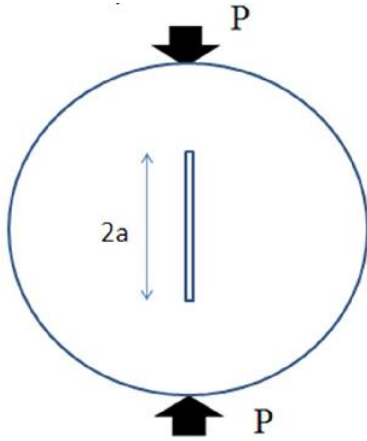
Fig. 5 Noched Brazilian disk specimen under diametrical compression

Fig. 6 SCB specimen geometry

Fig. 7 HCCD geometry

cm. A straight edge cracks with length of *a* is created from the surface of the disc. The tensile fracture toughness (*KIC*) for END specimen are written as

$$KIC = F\frac{P}{D}\sqrt{\pi a} \tag{6}$$

Where *P* is applied compression load and *F* is non-dimensional stress intensity factor. *YI* is depend on *a* and *D* and range from 0.1 to 0.6 (Table 1).

NBD test

Schematic view and geometrical dimension of NBD is presented in Fig. 5 (Atkinson *et al.* 1982). When a notched rock specimen is subjected to an externally applied load, stress concentrates in the vicinity of the crack tip. When this stress concentration reaches a critical value, failure occurs due to propagation of the pre-existing crack. The fracture toughness is then calculated in terms of the stress intensity factor (*SIF*) using the failure load, notch size, and other geometrical parameters of the specimen.

In this paper, a circular disk with a central vertical straight notch under diametrical compression was used to investigate fracture toughness. The following mathematical expressions, proposed by Atkinson *et al.* (1982), were used for the fracture toughness calculation

$$KI = \frac{P\sqrt{a}}{\sqrt{\pi}RB}NI \tag{7}$$

$$NI = 1 \tag{8}$$

Where *KI* is Mode-I stress intensity factor; *R* is radius of the Brazilian disk; *B* is thickness of the disk; *P* is compressive load at failure; a is half crack length; and, *NI* is non-dimensional coefficient which depend on a/R and (*β*) the orientation angle.

SCB test

The geometry of the SCB specimen is shown in Fig. 6. This test was developed by Chong and Kuruppu (2014). The SCB specimen is typically core-based and requires
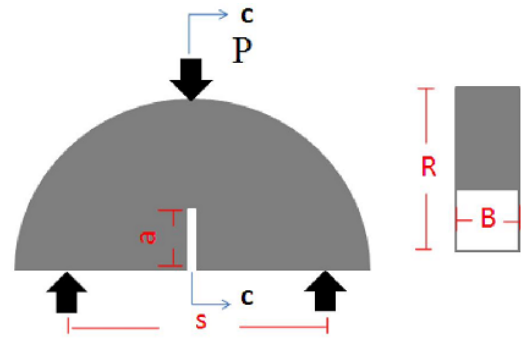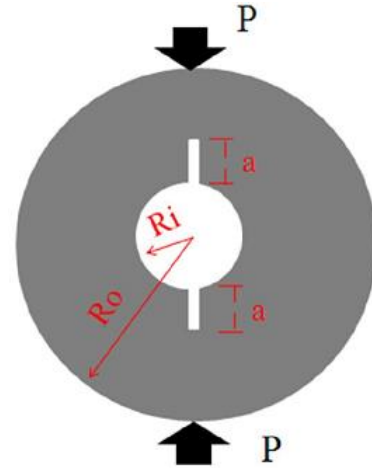
relatively little machining effort. In particular, its compact shape formed by cutting a core into slices and duplicated half semi-circular disks is suitable for conveniently investigating the effect of various parameters such as strain rate, moisture content, and temperature on the fracture toughness of rocks.

The mode I fracture toughness *KIc* is estimated using the following equation (Kuruppu *et al.* 2014)

$$KI = \frac{P\sqrt{\pi a}}{2rt}YI \tag{9}$$

$$YI = -1.297 + 9.516(\frac{S}{2R}) \tag{10}$$

where *a*, *r*, and *t* are an artificial notch length, radius, and thickness of the specimen, respectively. *P* is a maximum load. The normalized stress intensity factor *YI* is dimensionless and given as a function of a dimensionless notch length a/r and a half of the support span to radius ratio s/r (Kuruppu *et al.* 2014).

HCCD test

Schematic view and geometrical dimension of HCCD specimens is presented in Fig. 7(a) Shiryaev and Kotkis, 1982. As can be seen in Fig. 7(a), HCCD is a disc with radius of *Rₒ* in which a central hole with radius of *Rᵢ* is drilled. Two straight central cracks with length of a are created from the surface of the hole. Obviously, vertical

Table 2 Micro properties used to represent the rock

Parameter	Value
Type of particle	Disc
Density	3000
Minimum radius	0.27
Size ratio	1.56
Porosity ratio	0.08
Damping coefficient	0.7
Contact young modulus (GPa)	40
Stiffness ratio	1.7
Parallel bond radius multiplier	1
Young modulus of parallel bond	40
Parallel bond stiffness ratio	1.7
Particle friction coefficient	0.4
Parallel bond normal strength, mean (MPa)	26
Parallel bond normal strength, SD (MPa)	2
Parallel bond shear strength, mean (MPa)	26
Parallel bond shear strength, SD (MPa)	2

notches are associated with the case of pure mode I condition. The stress intensity factors (KI) mode I of for the HCCD specimen are often written as

$$KI = \frac{P}{t(R_o - R_i)}\sqrt{\pi a}YI \qquad (11)$$

$$YI = 0.62 \qquad (12)$$

where P is applied compressive load and t is the thickness of specimen; YI is two dimensionless stress intensity factors.

In this paper CT test, HCCQS test, NBD test, SCB test, HCCD test, SENRBB test and END test were performed for measuring the mode I fracture toughness of rock. By these tests, it was determined that which one of indirect fracture toughness is close to direct one.

2. Particle flow code3

The Particle Flow Code in two dimensions (Itasca 1999) is a discontinue code that represents a rock mass as an assemblage of circular disks continued by planar walls. A three dimensional (3-D) version of the code is also available in which the particles are spheres, however, only 2-D models will be discussed here. The distinct element method (Potyondy 1996, 2004) is used to model the forces and motions of the particles within the assembly. The particles move independently of one another and inter act only at contacts. They are assumed to be rigid (non-deformable) but overlap can occur at the contacts. Contacts are assumed to exist only at a point and not over some finite surface area as would be the case with fully deformable particles. The particles can be bonded together to simulate a competent rock. The contact bonds can be envisaged as a pair of elastic springs (or a point of glue) with constant normal and shear stiffness's acting at a point. The values assigned to these
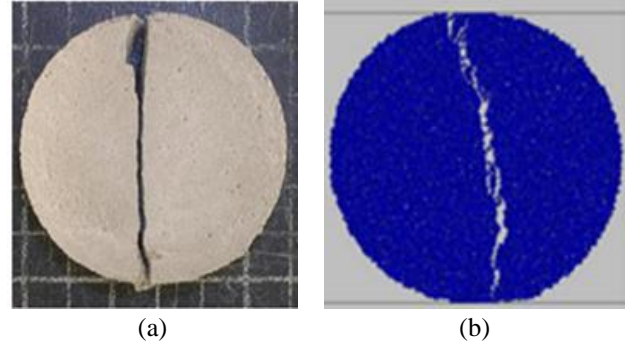

(a)   (b)

Fig. 8 Failure pattern in (a) physical sample, (b) PFC2D model

Table 3 Brazilian tensile strength of physical and numerical samples

Physical tensile strength (MPa)	4.6
Numerical tensile strength (MPa)	4.5

stiffness's influence the macro deformation properties of the rock sample (Young's modulus and Poisson's ratio). The contact bonds also have a specified shear and tensile strength. The values assigned to these strengths influence the macro strength of the sample and the nature of cracking and failure that occurs during loading. The contact bonds allow tension to exist at the contacts until the force at the contact exceeds the strength of the bond, at which time the bond breaks and the tensile force becomes zero. Similarly, the contact can support shear forces until the bond breaks, but in this case the shear force is set to a residual value that depends on the compressive normal force at the contact and the coefficient of friction. The contact behaviour is summarised in after a bond breaks in PFC, stress is redistributed and this may then cause more cracks to form nearby. If the rock model is suit ably stressed, then these bond breakages will localise into an inclined macro fracture eventually causing sample failure. In this way, deformation and fracture of rocks is modelled directly by allowing micromechanical damage to evolve, instead of indirectly by using constitutive equations as is the case in most continuum models. It has been shown that PFC can fairly accurately reproduce the fundamental mechanical behaviour of a range of rock types subjected to different stress regimes (Cundall 1979).

2.1 Model calibration

Brazilian test was used to calibrate the tensile strength of specimen in PFC2D model. Adopting the micro-properties listed in Table 2 and the standard calibration procedures (Potyondy and Cundall 1996), a calibrated PFC particle assembly was created. The diameter of the Brazilian disk considered in the numerical tests was 54 mm. The specimen was made of 5,615 particles. The disk was crushed by the lateral walls moved toward each other with a low speed of 0.016 m/s. The wall velocity was adequate low (0.016 m/s in all tests) to ensure a quasi-static equilibrium. Fig. 8(a), (b) illustrate the failure patterns of the numerical and experimental tested samples, respectively. The failure planes experienced in numerical and laboratory tests are
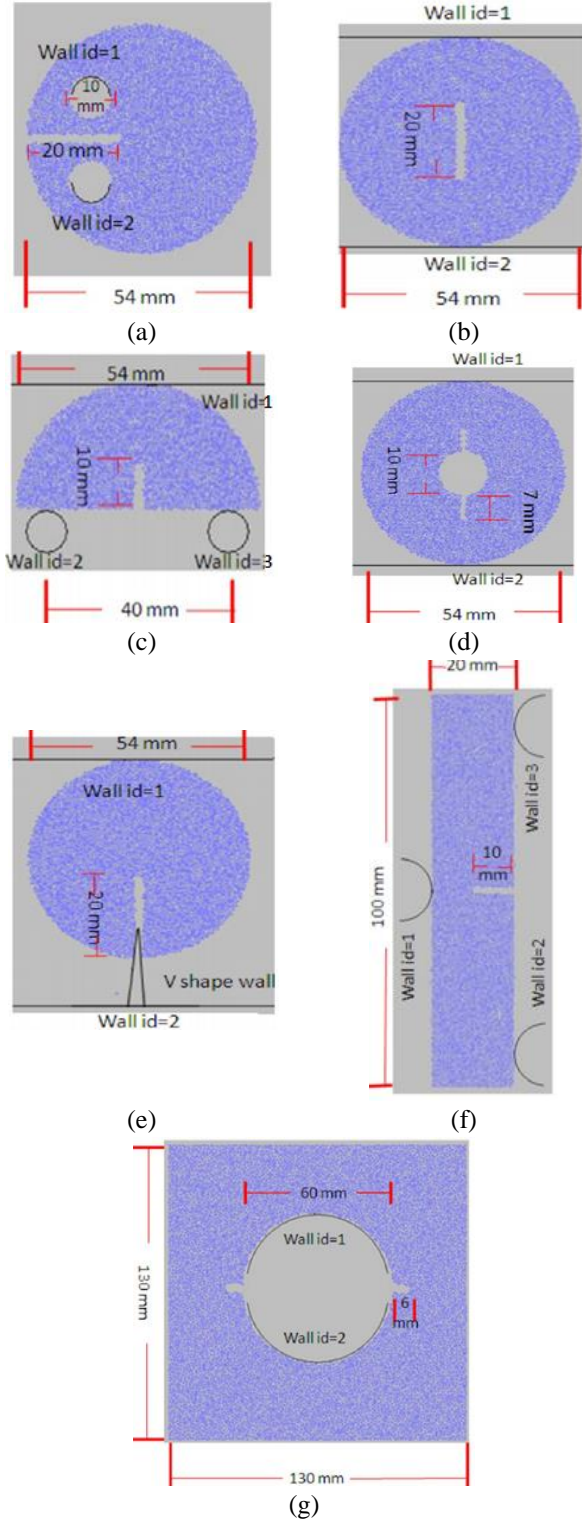
Fig. 9 Specification of numerical model, (a) CT test, (b) NBD test, (c) SBC test, (d) HCCD test, (e) END test, (f) SENRBB test and (g) HCCQS test

well matching. The numerical tensile strength and a comparison of its experimental measurements are presented in Table 3. This table shows a good accordance between numerical and experimental results.

2.2 CT test

After calibration of PFC2D, CT test was simulated by creating a model in the PFC2D (by using the calibrated micro-parameters) (Fig. 9(a)). The PFC specimen had dimensions of 75 mm×100 mm. A total of 11,179 disks with a minimum radius of 0.27 mm were used to make up the shear box specimen. Two rectangular zones with length of 30 mm and thickness of 20 mm, was removed from the right and left sides of the model. After model preparation, four loading wall were installed in contact with upper and lower sides of rectangular zones (Fig. 9(a)). Tensile loading was applied to the sample by moving the upper and lower walls in the positive side of Y-direction and in the opposite side of Y-direction, respectively. The Tensile force was registered by taking the reaction forces on the wall 3 in Fig. 9(a).

2.3 NBD test

The diameter of the NBD model considered in the numerical tests was 54 mm. One slit cut with length of 20 mm and opening of 1 mm was created vertically in center of the model. The specimen was made of 5,015 particles. The disk was crushed by the lateral walls moved toward each other with a low speed of 0.016 m/s. The wall velocity was adequate low (0.016 m/s in all tests) to ensure a quasi-static equilibrium. The crack initiation force was registered by taking the reaction forces on the wall 1 in Fig. 9(b).

2.4 SCB test

SCB Test was simulated by creating a semi-circle model in the PFC2D (by using the calibrated micro-parameters) (Fig. 9(c)). Diameter of model was 54 mm. one slit cut with length of 1 mm and opening of 1 mm was created in lower side of the model. The specimen was made of 2412 particles. After model preparation, three loading wall were installed in contact with the model (Fig. 9(c)).

The spacing between the lower walls was 40 mm. tensile loading was applied to the sample by moving the lower and upper walls in the positive side of Y-direction and in the opposite side of Y-direction, respectively. The disk was crushed by the loading walls moved toward each other. The crack initiation force was registered by taking the reaction forces on the wall 1 in Fig. 9(c).

2.5 HCCD test

HCCD test was simulated by creating a circle model in the PFC2D (by using the calibrated micro-parameters) (Fig. 9(d)). Diameter of the Ring disk was 54 mm. a circle with diameter of 10 mm was removed from the model. Two slit cut with length of 7 mm and opening of 1 mm was created in upper and lower sides of the hole. The specimen was made of 4312 particles. The disk was crushed by the loading walls moved toward each other. The crack initiation force was registered by taking the reaction forces on the wall 1 in Fig. 9(d).

2.6 END test

The diameter of the END model considered in the
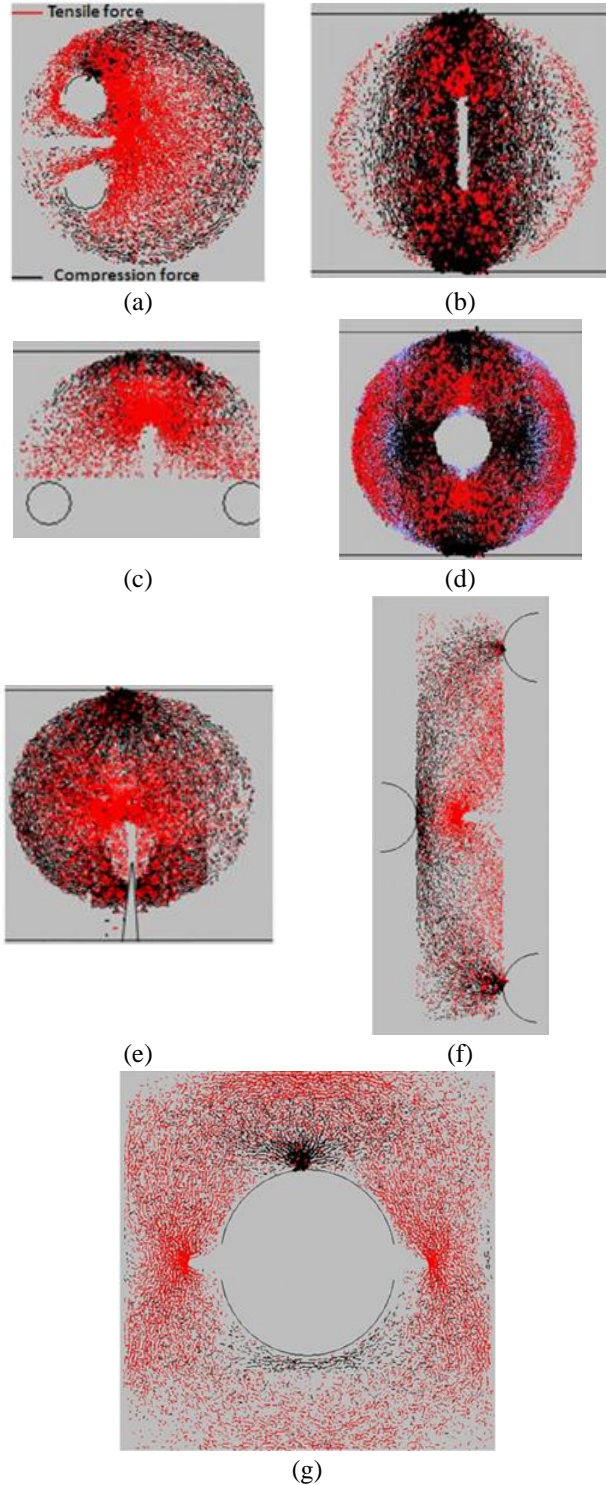
(a)

(b)

(c)

(d)

(e)

(f)

(g)

Fig. 10 Distribution of parallel bond forces in the models before the crack initiation occurs; (a) CT test, (b) NBD test, (c) SBC test, (d) HCCD test, (e) END test, (f) SENRBB test and (g) HCCQS test

numerical tests was 54 mm. One slit cut with length of 20 mm and opening of 1 mm was created vertically in lower sides and in the center of the model (Fig. 9(e)). The specimen was made of 5,015 particles. V shape loading wall was installed in the notch and two horizontal loading walls were installed in upper the model and lower the "V"

Shape wall, respectively. The disk was crushed by the horizontal walls moved toward each other with a low speed of 0.016 m/s. The crack initiation force was registered by taking the reaction forces on the horizontal wall (Fig. 9(e)).

2.7 SENRBB test

SENRBB Test was simulated by creating a box model in the PFC2D (by using the calibrated micro-parameters) (Fig. 9(f)). The PFC specimen had the dimensions of 1200 mm×20 mm. A total of 6326 disks with a minimum radius of 0.27 mm were used. One slit cut with length of 10 mm and opening of 1 mm was created in lower sides and in the middle of the model. After model preparation, three semi-circle loading walls were installed in contact with the model (Fig. 9(f)).

The spacing between the lower walls was 80 mm. tensile loading was applied to the sample by moving the lower and upper walls in the positive side of Y-direction and in the opposite side of Y-direction, respectively. The Tensile force was registered by taking the reaction forces on the wall 3 in Fig. 9(f).

2.8 HCCQS test

After calibration of PFC2D, CT test was simulated by creating a model in the PFC2D (by using the calibrated micro-parameters) (Fig. 9(g)). The PFC specimen had the dimensions of 13 mm×13 mm. A total of 11,179 disks with a minimum radius of 0.27 mm were used to make up the box specimen. A hole with radius of 6 cm is created in the centre of the model. Two straight central cracks with length of 6 mm and opening of 1mm are created from the surface of the hole. These cracks are perpendicular with loading axis (*P*). After model preparation, two semi-circle loading wall were installed in contact with upper and lower sides of hole (Fig. 9(g)). Tensile loading was applied to the sample by moving the upper and lower walls in the positive side of Y-direction and in the opposite side of Y-direction, respectively. The Tensile force was registered by taking the reaction forces on each wall (Fig. 9(g)).

3. Tensile failure mechanism

3.1 Parallel bond forces in the models before crack initiation

Fig. 10 shows the parallel bond force distribution at a state before the crack initiation in four PFC samples, which have different shapes. The dark and red lines represent the compression and tensile forces in the model, respectively. The coarser the line is, the larger the force is. As can be seen, the maximum force concentrations occur around the joint tips. It means that crack will initiated at tip of the joint.

3.2 Failure patterns in numerical models

Fig. 11(a), (b), (c), (d), (e), (f) and (g) shows progress of cracks in CT test, NBD test, SCB test, HCCD test, END test, SENRBB test and HCCQS test, respectively. Black

(a)   (b)

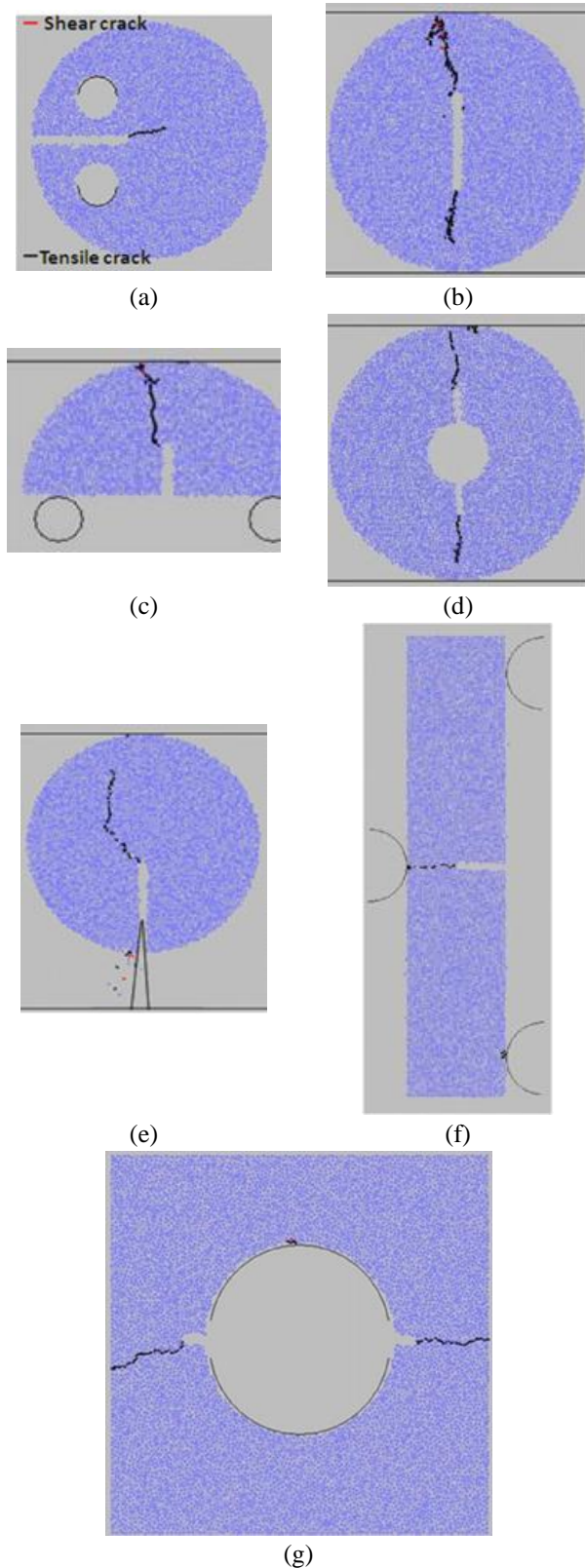(c)   (d)

(e)   (f)

(g)

Fig. 11 progress of cracks in (a) CT test, (b) NBD test, (c) SBC test, (d) HCCD test, (e) END test, (f) SENRBB test and (g) HCCQS test

lines and red lines represent the tensile cracks and shear cracks, respectively. Figs. 11(b), (c), (d), (e) and (f) shows that in NBD, SCB, HCCD, END and SENRBB tests, tensile

Table 4 Fracture toughness in different tests

Tested method	Fracture toughness (MPa$\sqrt{m}$)
CT	1.76
NBD	1.86
SCB	1.78
HCCD	1.91
END	1.78
SENRBB	1.79
HCCQS	1.74

cracks initiates from the joint tips, propagates parallel to the loading axis till coalesces to the sample edge. In CT test HCCQS tests, tensile cracks initiates from the joint tips, propagates perpendicular to the loading axis till coalesces to the sample edge (Figs. 11(a) and (g)). It's to be note that particle size has important effect on the crack growth trajectory. In all of the numerical models, balls diameters are more than physical particles diameters. Therefore the crack growth path is nearly different from natural crack growth i.e., crack line is not straight and along the original pre-existing notch.

3.3 Comparison between fracture toughness in numerical models

Table 4 shows a comparison between the Fracture toughness for CT, NBD, SCB, HCCD, END, SENRBB and HCCQS tests.

Results from numerical tests shows that direct test methods such as CT and HCCQS tests yields the lowest fracture toughness (Table 3) due to pure tensile stress distribution on failure surface (Fig. 7(d)). HCCD and NBD tests yields the highest fracture toughness values (Table 3). It is interesting to note that fracture toughness obtained from SCB and SENRBB tests are nearly equal to the direct test result. It's to be note that whereas sample preparation is difficult in SENRBB model therefore SCB test can be a proper test for determination of fracture toughness of rock in absence of direct tests. Other advantages shown by SCB tests are: (1) the SCB test need less sample size compared with other tests, (2) less material is need for sample preparation, (3) sample preparation is easy and (4) the use of a simple conventional compression press controlled by displacement compared with complicate device in other tests.

4. Conclusions

The fracture toughness of rock in direct test (CT and HCCQS) and indirect tests (NBD, SCB, HCCD, SENRBB and END tests) has been investigated using numerical simulations. By using numerical testing, the failure process was visually observed and different failure patterns were watched. Discrete element simulations demonstrated that the macro fractures in models are caused by microscopic tensile breakages on large numbers of bonded discs. Fracture toughness of rock in direct test was less than other

tests results. Fracture toughness resulted from SCB test was close to direct test result. So SCB can be a proper test for determination of fracture toughness of rock in absence of direct test. Other advantages shown by punch tests are: (1) the punch test need less sample size compared with other tests, (2) less material is need for sample preparation, (3) sample preparation is easy and (4) the use of a simple conventional compression press controlled by displacement compared with complicate device in other tests.

References

Akbas, S. (2016), "Analytical solutions for static bending of edge cracked micro beams", *Struct. Eng. Mech.*, **59**(3), 66-78.

Aliha, M.R. and Ayatollahi, M.R. (2013), "Two-parameter fracture analysis of SCB rock specimen under mixed mode loading", *Eng. Fract. Mech.*, **103**, 115-123.

Aliha, M.R. and Ayatollahi, M.R. (2014b), "Rock fracture toughness study using cracked chevron notched Brazilian disc specimen under pure modes I and II loading-a statistical approach", *Theor. Appl. Fract. Mech.*, **69**, 17-25.

Aliha, M.R., Ayatollahi, M.R. and Akbardoost, M.R.J. (2012b), "Typical upper bound-lower bound mixed mode fracture resistance envelopes for rock material", *Rock Mech. Rock Eng.*, **45**(1), 65-74.

Aliha, M.R., Ayatollahi, M.R. and Pakzad, R. (2008), "Brittle fracture analysis using a ring-shape specimen containing two angled cracks", *J. Fract.*, **153**(1), 63-68.

Aliha, M.R., Bahmani, A. and Akhondi, S. (2015a), "Determination of mode III fracture toughness for different materials using a new designed test configuration", *Mater. Des.*, **86**, 863-871.

Aliha, M.R., Bahmani, A. and Akhondi, S. (2015b), "Numerical analysis of a new mixed mode I/III fracture test specimen", *Eng. Fract. Mech.*, **134**, 95-110.

Aliha, M.R., Hosseinpour, G.R. and Ayatollahi, M.R. (2013), "Application of cracked triangular specimen subjected to three-point bending for investigating fracture behavior of rock materials", *Rock Mech. Rock Eng.*, **46**(5), 1023-1034.

Aliha, M.R., Pakzad, R. and Ayaollahi, M.R. (2014a), "Numerical analyses of a cracked straight-through flattened Brazilian disk specimen under mixed-mode loading", *J. Eng. Mech.*, **140**(1), 219-224.

Aliha, M.R.M., Sistaninia, M., Smith, D.J., Pavier, M.J., Ayatollahi, M.R. (2012a), "Geometry effects and statistical analysis of mode I fracture in guiting limestone", *J. Rock Mech. Min. Sci.*, **51**, 128-135.

Amrollahi, H., Baghbanan, A. and Hashemolhosseini, H. (2011), "Measuring fracture toughness of crystalline marbles under modes I and II and mixed mode I-II loading conditions using CCNBD and HCCD specimens", *J. Rock Mech. Min. Sci.*, **48**(7), 1123-1134.

Atkinson, B.K. (1987), Fracture Mechanics of Rock, Academic Press, London, U.K.

Atkinson, C., Smelser, R.E. and Sanchez, J. (1982), "Combined mode fracture via the cracked Brazilian disc test", *J. Fract.*, **18**(4), 279-291.

Ayatollahi, M.R. and Alborzi, M.J. (2013), "Rock fracture toughness testing using SCB specimen", *Proceedings of the 13th International Conference on Fracture*, Beijing, China, June.

Banks-Sills, L. and Bortman, Y. (1986), "A mixed mode fracture specimen: Analysis and testing", *J. Fract.*, **30**(3), 181-201.

Barker, L.M. (1977), "A simplified method for measuring plane strain fracture toughness", *Eng. Fract. Mech.*, **9**(2), 361-369.

Buchholz, F.G., Pirro, P.J.M., Richard, H.A. and Dreyer, K.H. (1987), "Numerical and experimental mixed-mode analysis of a compact tension-shear-specimen", *Proceedings of the 4th International Conference Numerical Methods in Fracture Mechanics*, Pineridge Press.

Chang, S.H., Lee, C.I. and Jeon, S. (2002), "Measurement of rock fracture toughness under modes I and II and mixed-mode conditions by using disc- type specimen", *Eng. Geol.*, **66**(1), 9-97.

Chong, K.P. and Kuruppu, M.D. (1984), "New specimen for fracture toughness determination for rock and other materials", *J. Fract.*, **26**(2), 59-62.

Chong, K.P., Kuruppu, M.D. and Kuszmaul, J.S. (1987), "Fracture toughness determination of layered materials", *Eng. Fract. Mech.*, **28**(1), 43-54.

Cundall, P.A. and Strack, O. (1979), "A discrete element model for granular assemblies", *Geotech.*, **29**(1), 47-65.

Dai, F., Chen, R., Iqbal, M.J. and Xia, K. (2010), "Dynamic cracked chevron notched Brazilian disc method for measuring rock fracture parameters", *J. Rock Mech. Min. Sci.*, **47**(4), 606-613.

Fayed, A.S. (2017), "Numerical analysis of mixed mode I/II stress intensity factors of edge slant cracked plates", *Eng. Sol. Mech.*, **5**(1), 61-70.

Hadei1, R. and Kemeny, J. (2016), "New development to measure mode I fracture toughness in rock", *Period. Polytech. Civil Eng.*, **61**(1), 51.

Haeri, H. (2015d), "Propagation mechanism of neighboring cracks in rock-like cylindrical specimens under uniaxial compression", *J. Min. Sci.*, **51**(3), 487-496.

Haeri, H. (2015e), "Influence of the inclined edge notches on the shear-fracture behavior in edge-notched beam specimens", *Comput. Concrete*, **16**(4), 605-623.

Haeri, H. (2015f), "Experimental crack analysis of rock-like CSCBD specimens using a higher order DDM", *Comput. Concrete*, **16**(6), 881-896.

Haeri, H. and Sarfarazi, V. (2016a), "The effect of micro pore on the characteristics of crack tip plastic zone in concrete", *Comput. Concrete*, **17**(1), 107-112.

Haeri, H., Khaloo, K. and Marji, M.F. (2015b), "Experimental and numerical analysis of Brazilian discs with multiple parallel cracks", *Arab. J. Geosci.*, **8**(8), 5897-5908

Haeri, H., Marji, M.F. and Shahriar, K. (2015a), "Simulating the effect of disc erosion in TBM disc cutters by a semi-infinite DDM", *Arab. J. Geosci.*, **8**(6), 3915-3927.

Haeri, H., Sarfarazi, V. and Lazemi, H. (2016b), "Experimental study of shear behavior of planar non-persistent joint", *Comput. Concrete*, **17**(5), 639-653.

Haeri, H., Shahriar, K., Marji, M.F. and Moarefvand, P. (2014), "Investigating the fracturing process of rock-like Brazilian discs containing three parallel cracks under compressive line loading", *Str. Mater.*, **46**(3), 133-148.

Haeri, H., Shahriar, K., Marji, M.F. and Moarefvand, P. (2015c), "The HDD analysis of micro cracks initiation, propagation and coalescence in brittle substances", *Arab. J. Geosci.*, **8**, 2841-2852.

He, M.Y., Cao, H.C. and Evans, A.G. (1990), "Mixed-mode fracture: The four point shear specimen", *Acta Metal Mater.*, **38**(5), 839-846.

Huang, J. and Wang, S. (1985), "An experimental investigation concerning the comprehensive fracture toughness of some brittle rocks", *J. Rock Mech. Min. Sci. Geomech. Abstr.*, **22**(2), 99-104.

Isida, M., Imai, R. and Tsuru, H. (1979), "Symmetric plane problems of arbitrarily shaped plates with an edge crack", *Trans. Jap. Soc. Mech. Eng.*, **45**(395A), 743-749.

ISRM (2007), The Complete ISRM Suggested Methods for Rock

Characterization Testing and Monitoring: 1974-2006, International Society for Rock Mechanics, Kozan Ofset, Ankara, Turkey.

Itasca PFC2D (1999), Particle Flow Code in 2 Dimensions, Theory and Background, Itasca Consulting Group, Minneapolis, U.S.A.

Karfakis, M.G. and Akram, M. (1993), "Effects of chemical solutions on rockm fracturing", *J. Rock Mech. Min. Sci. Geomech. Abstr.*, 30(7), 1253-1259.

Kataoka, M. and Obara, Y. (2013), "Estimation of fracture toughness of different kinds of rocks under water vapor pressure by SCB test", *J. MMIJ*, **129**, 425-432.

Kataoka, M., Hashimoto, A., Sato, A. and Obara, Y. (2012), "Fracture toughness of anisotropic rocks by semi-circular bend (SCB) test under water vapor pressure", *Proceedings of the 7th ARMS*, Seoul, Korea, October.

Kataoka, M., Obara, Y. and Kuruppu, M. (2011), "Estimation of fracture toughness of anisotropic rocks by SCB test and visualization of fracture by means of X-ray CT", *Proceedings of the 12th ISRM International Congress*, Beijing, China, October.

Kequan, Y.U. and Zhoudao, L.U. (2015), "Influence of softening curves on the residual fracture toughness of post-fire normal-strength concrete", *Comput. Concrete*, **15**(2), 102-111.

Khan, K. and Al-Shayea, N.A. (2000), "Effect of specimen geometry and testing method on mixed I-II fracture toughness of a limestone rock from Saudi Arabia", *Rock Mech. Rock Eng.*, **33**(3), 179-206.

Kuruppu, M.D., Obara, Y., Ayatollahi, M.R., Chong, K.P. and Funatsu, T. (2014), "ISRM-suggested method for determining the mode I static fracture toughness using semi-circular bend specimen", *Rock Mech. Rock Eng.*, **47**, 267-274.

Lee, S. and Chang, Y. (2015), "Evaluation of RPV according to alternative fracture toughness requirements", *Struct. Eng. Mech.*, **53**(6), 1271-1286.

Lim, I.L., Johnston, I.W. and Choi, S.K. (1993), "Stress intensity factors for semi-circular specimens under three-point bending", *Eng. Fract. Mech.*, **44**(3), 363-382.

Lim, I.L., Johnston, I.W., Choi, S.K. and Boland, J.N. (1994), "Fracture testing of a soft rock with semi-circular specimens under three-point loading, part 1-mode I", *J. Rock Mech. Min. Sci.*, **31**(3), 185-197.

Maccagno, T.M. and Knott, J.F. (1989), "The fracture behaviour of PMMA in mixed modes I and II", *Eng. Fract. Mech.*, **34**(1), 65-86.

Mahajan, R.V. and Ravi-Chandar, K. (1989), "An experimental investigation of mixed-mode fracture", *J. Fract.*, **41**(4), 235-252.

Mohammad, A. (2016), "Statistical flexural toughness modeling of ultra high performance concrete using response surface method", *Comput. Concrete*, **17**(4), 33-39.

Molenar, A.A.A., Scarpas, A., Liu, X. and Erkens, S.M.J.G. (2002), "Semi-circular bending test: Simple but useful?", *J. Assoc. Asph. Pav. Technol.*, **71**, 794-815.

Obara, Y., Kuruppu, M. and Kataoka, M. (2010), "Determination of fracture toughness of anisotropic rocks under water vapour pressure by semi-circular bend test", *Proceedings of the Mine Planning and Equipment Selection*, Victoria, Australia.

Obara, Y., Sasaki, K. and Yoshinaga, T. (2007), "Estimation of fracture toughness of rocks under water vapour pressure by semi-circular bend (SCB) test", *J. MMIJ*, **123**(4-5), 145-151.

Obara, Y., Yoshinaga, T. and Hirata, A. (2009), "Fracture toughness in mode I and II of rock under water vapour pressure", *Proceedings of the ISRM Regional Symposium EUROCK*, Cavtat, Italy.

Ouchterlony, F. (1980), A New Core Specimen for the Fracture Toughness Testing of Rock, Swedish Detonic Research Foundation Report, Stockholm, Sweden.

Ouchterlony, F. (1981), Extension of the Compliance and Stress Intensity Formulas for the Single Edge Crack Round Bar in Bending, ASTM STP 745.

Ouchterlony, F. (1986), "Suggested methods for determining the fracture toughness of rock", *J. Rock Mech. Min. Sci. Geo-Mech. Abstr.*, **25**(1), 71-96.

Ouchterlony, F. (1988), "Suggested methods for determining the fracture toughness of rock", *J. Rock Mech. Min. Sci. Geomech. Abstr.*, **25**(2), 71-96.

Pan, B., Gao, Y. and Zhong, Y. (2014), "Theoretical analysis of overlay resisting crack propagation in old cement concrete pavement", *Struct. Eng. Mech.*, **52**(4), 167-181.

Potyondy DO, Cundall PA (2004), "A bonded-particle model for rock", *J. Rock Mech. Min. Sci.*, **41**(8), 1329-1364.

Potyondy, D.O., Cundall, P.A. and Lee, C. (1996), "Modeling of rock using bonded assemblies of circular particles", *Proceedings of 2nd North American Rock Mechanics Symposium*, Montreal, Vancouver.

Rajabi, M., Soltani, N. and Eshraghi, I. (2016), "Effects of temperature dependent material properties on mixed mode crack tip parameters of functionally graded materials", *Struct. Eng. Mech.*, **58**(2), 144-156.

Ramadoss, P. and Nagamani, K. (2013), "Stress-strain behavior and toughness of high-performance steel fiber reinforced concrete in compression", *Comput. Concrete*, **11**(2), 55-65.

Sato, K. (2006), "Fracture toughness evaluation based on tension-softening model and its application to hydraulic fracturing", *Pure Appl. Geophys.*, **163**(5), 1073-1089.

Shiryaev, A.M. and Kotkis, A.M. (1982), "Methods for determining fracture toughness of brittle porous materials", *Industr. Labor.*, **48**(9), 917-918.

Singh, R.N. and Sun, G.X. (1990), "A numerical and experimental investigation for determining fracture toughness of welsh limestone", *Min. Sci. Technol.*, **10**(1), 61-70.

Suresh, S. and Shih, C.F., Morrone, A. and O'Dowd, N.P. (1990), "Mixed-mode fracture toughness of ceramic materials", *J. Am. Ceram. Soc.*, **73**(5), 1257-1267.

Tutluoglu, L. and Keles, C. (2011), "Mode I fracture toughness determination with straight notched disk bending method", *J. Rock Mech. Min. Sci.*, **48**(8), 1248-1261.

Zhou, Y.X., Xia, K., Li, X.B., Li, H.B., Ma, G.W., Zhao, J., Zhou, Z.L. and Dai, F. (2012), "Suggested methods for determining the dynamic strength parameters and mode-I fracture toughness of rock materials", *J. Rock Mech. Min. Sci.*, **49**, 105-112.

CC